 doi:10.20944/preprints201910.0161.v1

Article

Enterovirus 71 Represses Interleukin Enhancer Binding Factor 2 Production and Nucleus Translocation to Antagonize ILF2 Antiviral Effects

Jing Jin[1], Wenbiao Wang[2], Sha Ai[1], Qi Zhang[1], Kailang Wu[1], Yingle Liu[1,2], and Jianguo Wu[1,2,*]

[1]State Key Laboratory of Virology, College of Life Sciences, Wuhan University, Wuhan 430072, China;
[2]Guangdong Key Laboratory of Virology, Institute of Medical Microbiology, Jinan University, Guangzhou 510632, China.
***Correspondence:** E-mail: jwu@whu.edu.cn; Tel.: +86-27-68754979

Abstract: Enterovirus 71 (EV71) infection hand-foot-mouth disease (HFMD), meningoencephalitis, neonatal sepsis, and even fatal encephalitis in children, thereby representing a serious public health hazard. It is important to determine the mechanisms underlying the regulation of EV71 infection. In this study, we initially reveal that the interleukin enhancer binding factor 2 (ILF2) down-regulates EV71 50% tissue culture infective dose (TCID50), attenuates EV71 plaque formation unit (PFU), thereby repressing EV71 infection. Moreover, we reveal a distinct mechanism by which EV71 antagonizes ILF2-mediated antiviral effects. Chip data analyses show that ILF2 mRNA is reduced upon EV71 infection. Cellular studies indicate that EV71 infection represses ILF2 mRNA expression and protein production in human leukemic monocytes (THP-1) differentiated macrophages and in human rhabdomyosarcoma (RD) cells. Additionally, EV71 non-structural protein 2B interacts with ILF2 in human embryonic kidney (HEK293T) cells. Interestingly, in the presence of EV71 2B, ILF2 is translocated from the nucleus to the cytoplasm and co-localizes with 2B in the cytoplasm. Therefore, we reveal a distinct mechanism by which EV71 antagonizes ILF2-mediated antiviral effects by inhibiting ILF2 expression and promoting ILF2 translocation from the nucleus to cytoplasm through its 2B protein.

Keywords: Enterovirus 71; EV71; EV71 non-structural protein 2B; Interleukin enhancer binding factor 2; ILF2; Virus infection; Virus replication.

1. Introduction

Enterovirus 71 (EV71), a positive-stranded RNA virus, is a member of Enterovirus within the family Picornaviridae [1, 2]. EV71 infection may cause hand-foot-mouth disease (HFMD), meningoencephalitis, neonatal sepsis, and fatal encephalitis in children [3, 4]. The viral genome contains a signal-stranded positive-sense RNA with one open reading frame (ORF) that encodes a polyprotein of approximately 250-kDa carrying three regions named P1, P2, and P3 [5]. Upon EV71 infection, the protein precursor is cleaved into 4 structural proteins (VP1, VP2, VP3, and VP4) and 7 non-structural proteins (2A, 2B, 2C, 3A, 3B, 3C, and 3D) [6]. Among the proteins, 2B is involved in EV71 RNA replication [7], localizes to the mitochondria to activate the mitochondrial cell death [8], enhances viral release [9], and antagonizes retinoic acid-inducible gene I (RIG-I)-mediated antiviral effects [10].

Interleukin enhancer binding factor 2 (ILF2) is a transcriptional activator to regulate interleukin 2 (IL-2) expression [11]. ILF2 together with its binding partner ILF3 regulates DNA replication [12, 13], transcription [14], translation [15, 16], mRNA splicing [17], and micro-RNA biogenesis [18–20]. ILF2 is also participated in the progression of pancreatic carcinoma [21, 22], hepatocellular carcinoma [20, 23], lung cancer [24], oesophageal squamous cell carcinoma [25], gastric cancer [26], and breast cancer [27]. Moreover, ILF2 regulates the replication of immunodeficiency virus type 1 (HIV-1) [28], hepatitis C virus (HCV) [29], rhinovirus type 2 (ERV-2) [30], white spot syndrome virus

 doi:10.20944/preprints201910.0161.v1

(WSSV) [31], human papilloma virus (HPV) [32], and respiratory syndrome virus (RSV) [33]. However, the mechanisms underlying the control of ILF2-mediated antiviral effects are not reported, and the role of ILF2 in EV71 replication is unknown.

Recently, we demonstrated that EV71 non-structural protein 3D (also known as *RNA-dependent RNA* polymerase, RdRP) binds to the NACHT, LRR and PYD domains-containing protein 3 (NLRP3, the sensor component of NLRP3 inflammasome) to enhance the inflammasome activation [34], and revealed that ILF2 interacts with NLRP3 to inhibit the inflammasome activation [35]. These results suggest that ILF2 may play roles in EV71 infection. Here, we show that ILF2 reduces EV71 50% tissue culture infective dose (TCID50) and plaque forming unit (PFU), providing the first evidence that ILF2 represses EV71 infection. In another hand, EV71 represses ILF2 mRNA expression and protein production. Additionally, EV71 non-structural protein 2B interacts with ILF2 to facilitate ILF2 translocated from nucleus to cytoplasm and promote 2B-ILF2 co-localization in cytoplasm. Therefore, we reveal a distinct mechanism by which EV71 antagonizes ILF2-mediated antiviral effects by inhibiting ILF2 expression and promoting ILF2 translocation from the nucleus to cytoplasm through 2B protein.

2. Materials and Methods

2.1. Reagents

Phorbol-12-myristate-13-acetate (TPA) (#P8139), murine monoclonal HA antibody (H6908), anti-glyceraldehyde-3-phosphate dehydrogenase (GAPDH) antibodies (#G9295), and Methyl cellulose (CMC-nZVI) (101839688) were purchased from Sigma (Sigma, St. Louis, MO). RPMI 1640 medium, Delbecco modified Eagle medium (DMEM), and fetal bovine serum (FBS) were purchased from Gibco (Grand Island, NY). anti-ILF2 were purchased from Santa Cruz (SC-365283) (Santa Cruz Biotechnology, Santa Cruz, CA). Anti-EV71 3C antibody (#A10003) and Murine monoclonal Green fluorescent protein (GFP) antibody (#AE012) were purchased from ABclonal (ABclonal Technology, Wuhan, China). Protease inhibitor Cocktail (#04693132001) were purchased from Roche (Pleasanton, CA, USA). Protein markers (#26616) were purchased from Fermentas (Burlington, Ontario, Canada). Polyvinylidene fluoride (PVDF) membranes (#IPVH00010) were purchased from Millipore (Millipore Corporation, Bedford, MA). FITC-conjugated anti-mouse antibodies (#133702A) and Dylight 649-conjugated anti-rabbit secondary antibodies (#ATPSE2901) were purchased from Abbkine (San Diego, CA). Bovine serum albumin (BSA) (#B0014K061000) were purchased from Biosharp (Hefei, China).

2.2. Cell Lines

Human embryonic kidney (HEK293T) cells, African green monkey kidney epithelial (Vero) cells, human rhabdomyosarcoma (RD) cells, and human leukemic monocyte (THP-1) cells were purchased from American Tissue Culture Collection (ATCC). Cells were cultured in DMEM supplemented with 10% FBS, 100 U/ml penicillin, and 100 μg/ml streptomycin at 37°C under 5% CO_2.

2.3. Stimulation of THP-1 Cells and Differentiation into Adherent Macrophages

THP-1 cells were differentiated into macrophages under the stimulation of 60 nM TPA. TPA was withdraw in 12–16 h and cells were cultured for additional 24 h.

2.4. Plasmid Construction

The EV71 genome fragments encoding 2B, 3C, 3A, 3C, and 3D protein were respectively cloned into pEGFPC1 between *Hind*III and *Sal*I sites, resulting in green fluorescent protein (GFP) fusion protein. The ILF2 gene was cloned into pCaggs-HA between *Eco*RI and *Xho*I sites.

2.5. Lentivirus Construction

 doi:10.20944/preprints201910.0161.v1

GFP protein on pLenti CMV GFP Puro vector (#17448) (Addgene, Watertown, MA) was replaced with a 3 × FLAG sequence and some stringent restriction sites (*Xba*I, *Eco*RV, *Bst*BI, and *BamH*I) were added before the FLAG tag. ILF2 gene was constructed into pLenti vector, and then it was transfected into HEK293T cells with psPAX2 (#12260) (Addgene) and PMD2.G (#12259) (Addgene) plasmid *via* Lipo 2000 (52887) (Invitrogen, Carlsbad, CA). The primers used were 5′-CTAGTCTAGAATGAGGGGTGACAGAGGCCG-3′ and 5′-GGAAGATCTCTCCTGAGTTTCCATGCTTTC-3′. Supernatants of transfected cells were collected after 36h incubation and used to infect RD cells with 4 μg/ml polybrene (#H9268) (Sigma). After 48 h of culture, the transduced cells were screened under the selection medium with 2.5 μg/ml puromycin (Sigma). Transgenic protein expression was analyzed by Western-blotting.

2.6. Real-Time PCR

Total RNA was isolated using TRIzol reagent (#15596018) (Invitrogen) in accordance with manufacturer's instructions and complementary DNA was synthesized using M-MLV Reverse Transcriptase(#M1705) (Promega) in accordance with manufacturer's instructions. Quantitative real-time RT–PCR analysis was performed using the Roche LC480 and SYBR RT-PCR kits (DBI Bio-science, Ludwigshafen, Germany). Real-time PCR primers were designed by Primer Premier 5.0 and their sequences were as follows: ILF2 forward, 5′-GATAATCTGATTGTGGCTCC-3′, ILF2 reverse, 5′-CGTTGGCAGAATCTTGAGTA-3′; GAPDH forward, 5′-AAGGCTGTGGGCAAGG-3′, GAPDH reverse, 5′-TGGAGGAGTGGGTGTCG-3′.

2.7. Western-Blotting

RD cells were lysed using lysis buffer: 50 mM Tris-HCl, pH7.5, 300 mM NaCl, 1% Triton-X, 5 mM EDTA, and 10% glycerol and protein was quantitated by Bradford method (Bio-Rad, Hercules, CA). Quantified samples were run on 10 SDS-PAGE gels and transferred onto Immobilon-P Transfer Membranes (PVDF) (Millipore, MA) using a transfer device. After blocking, PVDF membranes were incubated with primary antibodies overnight at 4°C, and then incubated with secondary antibodies at room temperature for 2 h. Blots were developed using chromogenic solution on Chemi-luminescence instrument (Fujifilm LAS-4000).

2.8. 50 % Tissue Culture Infective Dose (TCID50) Assay

Vero cells grown in 96-well plates to 90% confluence and inoculated with the supernatants from infected-RD cells for 2 h. Cells were washed with phosphate buffer saline (PBS) and cultured with 2% FBS in DMEM. At day 3 post-infection, the plates were examined for the lowest dilution at which 50% of the wells occurred the cytopathic effect (CPE).

2.9. Plaque Assay

The supernatant collected from infected RD cells was added to 12-well plate containing Vero cells at about 90% confluence. After 2 h incubation, the cells were washed with PBS and then 1 ml of plaque medium supplemented with 1% carboxylmethylcelluose (CMC-nZVI) was added to each well immediately. The plate was incubated at 37°C for 3 days. After the incubation, plaque medium was removed and cells were fixed and stained with 4% formaldehyde and 0.5% crystal violet.

2.10. Co-Immunoprecipitation (Co-IP)

HEK293T cells were lysed using lysis buffer at 4°C for 1 h, and anti-GFP antibody was added to the lysates for overnight incubation at 4°C. Protein-G (#14001578-EE) (GE Healthcare) was added to lysates and incubated for an additional 2 h. Immunocomplexes were washed with cell lysis buffer for 3 times and subsequently boiled in 2 X loading buffer for 10 min. Proteins were detected by Western-blotting as described.

2.11. Confocal Microscopy

 doi:10.20944/preprints201910.0161.v1

Plasmid-transfected HEK239T cells were fixed with 4% paraformaldehyde for 15 min at room temperature, permeabilized with 0.2% Triton-X100 for 5 min and blocked with 5% BSA for 1 h. Murine monoclonal GFP and HA antibody were added to cells for overnight incubation at 4°C and then FITC-conjugated anti-mouse and dylight 649-conjugated anti-rabbit secondary antibodies were incubated with cells for 1 h. Finally, cells were stained with DAPI for 5 min and confocal imaging was performed using Fluo View FV1000 (Olympus, Tokyo, Japan).

2.12. Statistical Analyses

All values are expressed as the mean ± SEM. Statistical analysis were performed with the t test for two groups or one-way ANOVA (GraphPad Prism5) for multiple groups. P values less than 0.05 were considered statistically significant.

3. Results

3.1. ILF2 represses EV71 infection in RD cells

The role of ILF2 in the regulation of EV71 infection was initially determined. Two recombinant lentiviruses, ILF2-lentivirus and its control CT-lentivirus, were constructed based on the procedures described previously [36]. Human rhabdomyosarcoma (RD) cells were infected with CT-lentivirus and ILF2-lentivirus to generate two stable cell lines. A basial level of endogenous ILF2 was detected in CT-lentivirus-cells, while a significantly higher level of ILF2 was produced in ILF2-lentivirus-cells (Figure 1A), indicating that ILF2 is stably expressed in ILF2-lentivirus-cells. Upon EV71 infection. EV71 3C was attenuated in ILF2-lentivirus-cells as compared with CT-lentivirus-cells (Figure 1B), demonstrating that ILF2 represses EV71 replication. Additionally, the cells were infected with EV71 and the supernatants were collected for 50% tissue culture infective dose (TCID50) assays. EV71 TCID50 was significantly down-regulated in ILF2-lentivirus-cells as compared with CT-lentivirus-cells (Figure 1C), indicating that ILF2 inhibits EV71 infection. Moreover, the cells were infected with EV71 and the supernatants were collected for plaque formation assays. Plaque formation unit (PFU) was remarkedly attenuated in ILF2-lentivirus-cells as compared with CT-lentivirus-cells (Figure 1D and E), suggesting that ILF2 attenuates EV71 infection. Therefore, these data provide the first evidence that ILF2 represses EV71 infection.

Preprints (www.preprints.org) | NOT PEER-REVIEWED | Posted: 15 October 2019 doi:10.20944/preprints201910.0161.v1

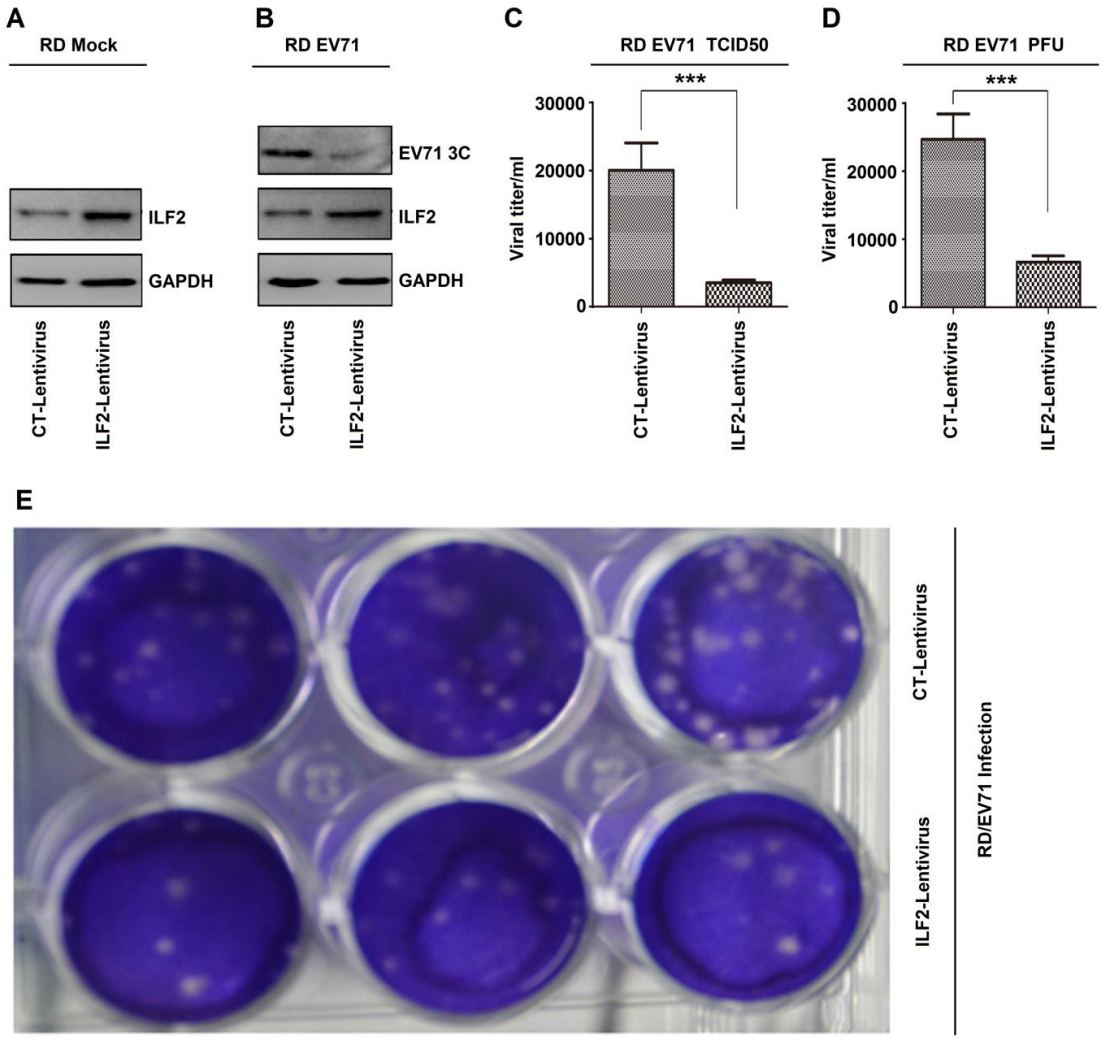

Figure 1. ILF2 represses EV71 infection in RD cells. (**A**) RD cells were infected with the recombinant lentiviruses, ILF2-lentivirus expressing ILF2 and its control CT-lentivirus, to generate two stable cell lines. ILF2 and GAPDH proteins expressed in the lysates of stable cell lines were detected by Western blot analysis. (**B**) The two stable cell lines were infected with EV71 (MOI = 0.5) for 12 h. ILF2, EV71 3C, and GAPDH proteins expressed in the lysates of stable cell lines were detected by Western blot analysis. (**C–E**) The stable cell lines were infected with EV71 (MOI = 0.5) for 12 h and the supernatants of cell cultures were collected and then inoculated into Vero cells. The levels of EV71 TCID50 were determined by TCID50 assays (C), the levels of EV71 PFU were determined by plaque assays (D), and visualized under confocal microscope (E).

3.2. ILF2 expression is attenuated in EV71-infected cells

Next, we determined whether EV71 plays any role in the regulation of ILF2. Differential mRNA expression of intracellular genes in EV71- or mock-infected RD cells were initially evaluated through Chip analyses. Z-score analyses of the Chip data showed that in EV71-infected cells, high mobility group box 2 (HMGB2), ILF2, proliferation-associated 2G4 (PA2G4), cyclin dependent kinase 2 associated protein 1 (CDK2AP1), calmodulin 2 (CALM2), cyclin dependent kinase 6 (CDK6), heterogeneous nuclear ribonucleoprotein H1 (HNRNPH1), Myc proto-oncogene protein (MYC), immediate early response 3 (IER3), dynein light chain LC8-type 1 (DYNLL1), far upstream element binding protein 1 (FUBP1), histone cluster 1 H4 family member e (HIST1H4E), and polo like kinase 2 (PLK2) were down-regulated, while the growth differentiation factor 15 (GDF15), seryl-tRNA synthetase (SARS), and macrophage migration inhibitory factor (MIF) were up-regulated (Figure 2A). Protein Analysis Through Evolutionary Relationships (PANTHER) revealed that

Preprints (www.preprints.org) | NOT PEER-REVIEWED | Posted: 15 October 2019 doi:10.20944/preprints201910.0161.v1

cholecystokinin receptor (CCKR) pathway, platelet-derived growth factor (PDGF) signaling, oxidative stress response (OSR), B-cell activation, interleukin signaling, Huntington disease (HD), Wnt pathway, heterotrimeric G-protein signaling pathway-rod outer segment (ROS), heterotrimeric G-protein signaling pathway-Gi alpha subunit, and Gi alpha mediated pathway, p53 pathway positive and negative feedback loops 2, T-cell activation, and transforming growth factor-β (TGF-β) signaling pathway were involved (Figure 2B). The basic functions of the proteins were summarized (Figure 2C). Therefore, Chip analyses reveal that ILF2 expression is attenuated in EV71-infected cells.

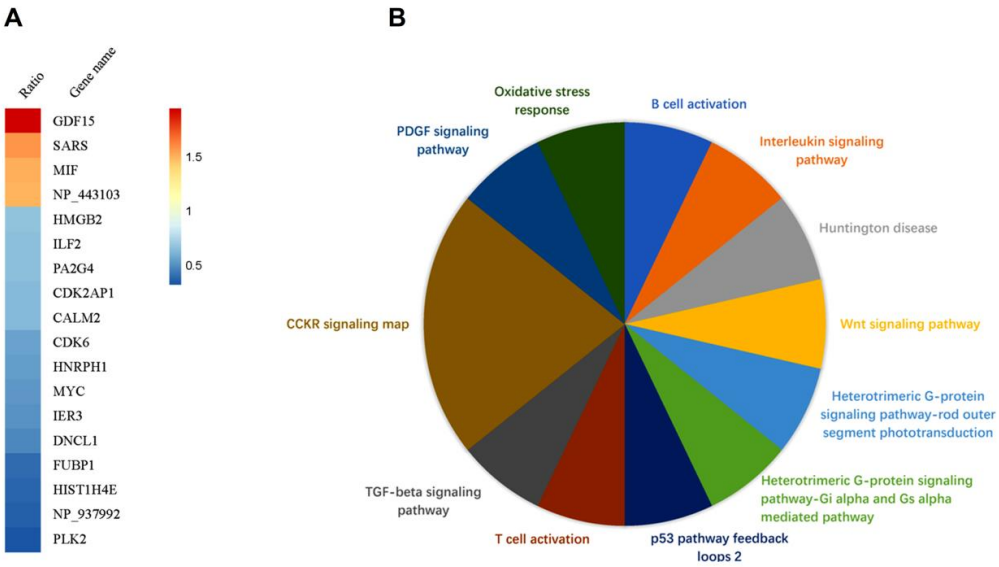

C

	Ensembl gene ID	Gene name	Function	Relative variation
1	ENSG00000130513	GDF15	stress response program after cellular injury	Up-regulation
2	ENSG00000031698	SARS	catalyzes the transfer of L-serine to tRNA (Ser)	Up-regulation
3	ENSG00000099964	MIF	suppress anti-inflammatory effects of glucocorticoids	Up-regulation
4	ENSG00000184943/ ENSG00000172965	NP_443103	cell proliferation and epithelial-mesenchymal transition	Up-regulation
5	ENSG00000164104	HMGB2	DNA circles and flexibility	Down-regulation
6	ENSG00000143621	ILF2	interleukin 2 gene expression and viral infection	Down-regulation
7	ENSG00000170515/ ENSG00000178116	PA2G4	RNA-binding and growth regulation.	Down-regulation
8	ENSG00000111328	CDK2AP1	negatively regulate CDK2 activity	Down-regulation
9	ENSG00000143933	CALM2	negatively regulate CDK2 activity,cell cycle and cell differentiation	Down-regulation
10	ENSG00000105810	CDK6	cell cycle and cell proliferation	Down-regulation
11	ENSG00000169045	HNRPH1	pre-mRNA processing,mRNA metabolism and transport	Down-regulation
12	ENSG00000136997	MYC	cell cycle progression, apoptosis and cellular transformation	Down-regulation
13	ENSG00000137331	IER3	TNF-αinduced apoptosis	Down-regulation
14	ENSG00000088986	DNCL1	intracellular transport and motility	Down-regulation
15	ENSG00000162613	FUBP1	DNA-binding	Down-regulation
16	ENSG00000197061	HIST1H4E	nucleosome structure of the chromosomal fiber	Down-regulation
17	ENSG00000111011	NP_937992	cell proliferation and survival	Down-regulation
18	ENSG00000145632	PLK2	cell division	Down-regulation

Figure 2. ILF2 expression is attenuated in EV71-infected cells. (**A**) The levels of differentially expressed gene mRNAs were analyzed by microarrays of RD cells infected with or without EV71(MOI = 0.5) for 12 h. Z-score analyses were used to choose the significant differentially

Preprints (www.preprints.org) | NOT PEER-REVIEWED | Posted: 15 October 2019 doi:10.20944/preprints201910.0161.v1

expressed genes. The mRNAs of genes with more than 1.5-fold variations of expression levels were defined as differentially expressed genes. Intensity ratio (experimental group/control group) of genes was calculated and visualized in R software (version 3.4.4) with Pheatmap Packages (version 1.0.8). (**B**) Differentially expressed genes were imported to PANTHER (Protein ANalysis THrough Evolutionary Relationships) Classification System to conduct Pathway analysis. (**C**) Summary of Ensembl gene IDs, gene names, functions, and relative variations of the differentially expressed genes.

3.3. EV71 represses ILF2 mRNA expression and protein production

Next, the role of EV71 in the regulation of ILF2 expression was determined in human leukemic monocytes (THP-1) cells and *RD cells*. THP-1 cells were differentiated into macrophages by stimulating with 12-o-tetradecanoylphorbol-13-acetate (TPA) as descripted previously [37, 38]. ILF2 mRNA was down-regulated upon EV71 infection in THP-1 differentiated macrophages (Figure 3A). Similarly, ILF2 mRNA was attenuated by EV71 infection in RD cells (Figure 3B). These results are consistent with the Chip data and demonstrate that EV71 infection represses ILF2 mRNA expression. Moreover, ILF2 protein was down-regulated and EV71 3C protein was produced in EV71-infected *RD cells* (Figure 3C), suggesting that EV71 attenuates ILF2 protein production. Taken together, we demonstrate that EV71 represses ILF2 mRNA expression and protein production.

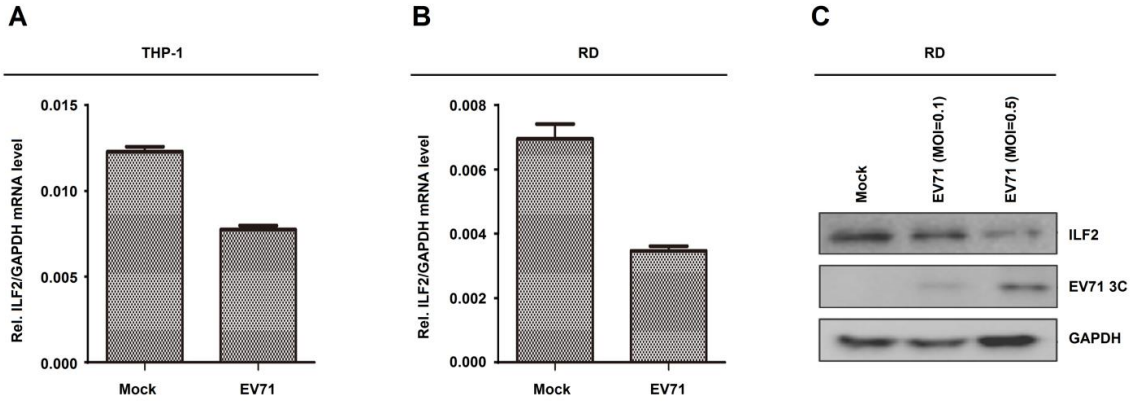

Figure 3. EV71 represses ILF2 mRNA expression and protein production. (**A**) THP-1 cells were differentiated into macrophages by stimulating with 12-o-tetradecanoylphorbol-13-acetate (TPA). TPA-differentiated THP-1 macrophages were infected with or without EV71(MOI=5) for 36 h. The mRNA level of ILF2 gene was quantified by real-time PCR. (**B**) RD cells were infected with or without EV71 (MOI = 1) for 12 h. The mRNA level of ILF2 gene was quantified by real-time PCR. (**C**) RD cells were infected with or without EV71 (MOI = 0.1 or 0.5) for 12 h. ILF2, EV71 3C, and GAPDH proteins expressed in the cell lysates were detected by Western blot analysis.

3.4. EV71 2B interacts and co-localizes with ILF2 in the cytoplasm

To further evaluate the effect of EV71 on the regulation of ILF2, the interactions among EV71 proteins and ILF2 were determined. Human embryonic kidney (HEK293T) cells were co-transfected with plasmid encoding HA-ILF2 and plasmids encoding each of EV71 non-structure proteins, GFP-2B, GFP-2C, GFP-3A, GFP-3C, and GFP-3D. Co-immunoprecipitation (Co-IP) results showed that EV71 2B interacted with ILF2, while other EV71 proteins failed to interact with ILF2 (Figure 4A). Additionally, 2B interacted with ILF2 (Figure 4B) and ILF2 associated with 2B (Figure 4C) in HEK293T cells, confirming the interaction between 2B and ILF2. Since 2B distributes in the cytoplasm [8], while ILF2 locates in the nucleus [33], we determined whether 2B co-localizes with ILF2 in HEK293T cells. Laser scanning confocal microscope showed that 2B (green) alone mainly localized in the cytoplasm (Figure 4D, top panels), ILF2 (red) alone majorly distributed in the nucleus (Figure 4D, middle panels), however, in the presence of both proteins, 2B and majority ILF2 were co-localized in the cytoplasm to form spots (Figure 4D, bottom panels). These results suggest that ILF2 is translocated from nucleus to the cytoplasm in the presence of EV71 2B.

Preprints (www.preprints.org) | NOT PEER-REVIEWED | Posted: 15 October 2019 doi:10.20944/preprints201910.0161.v1

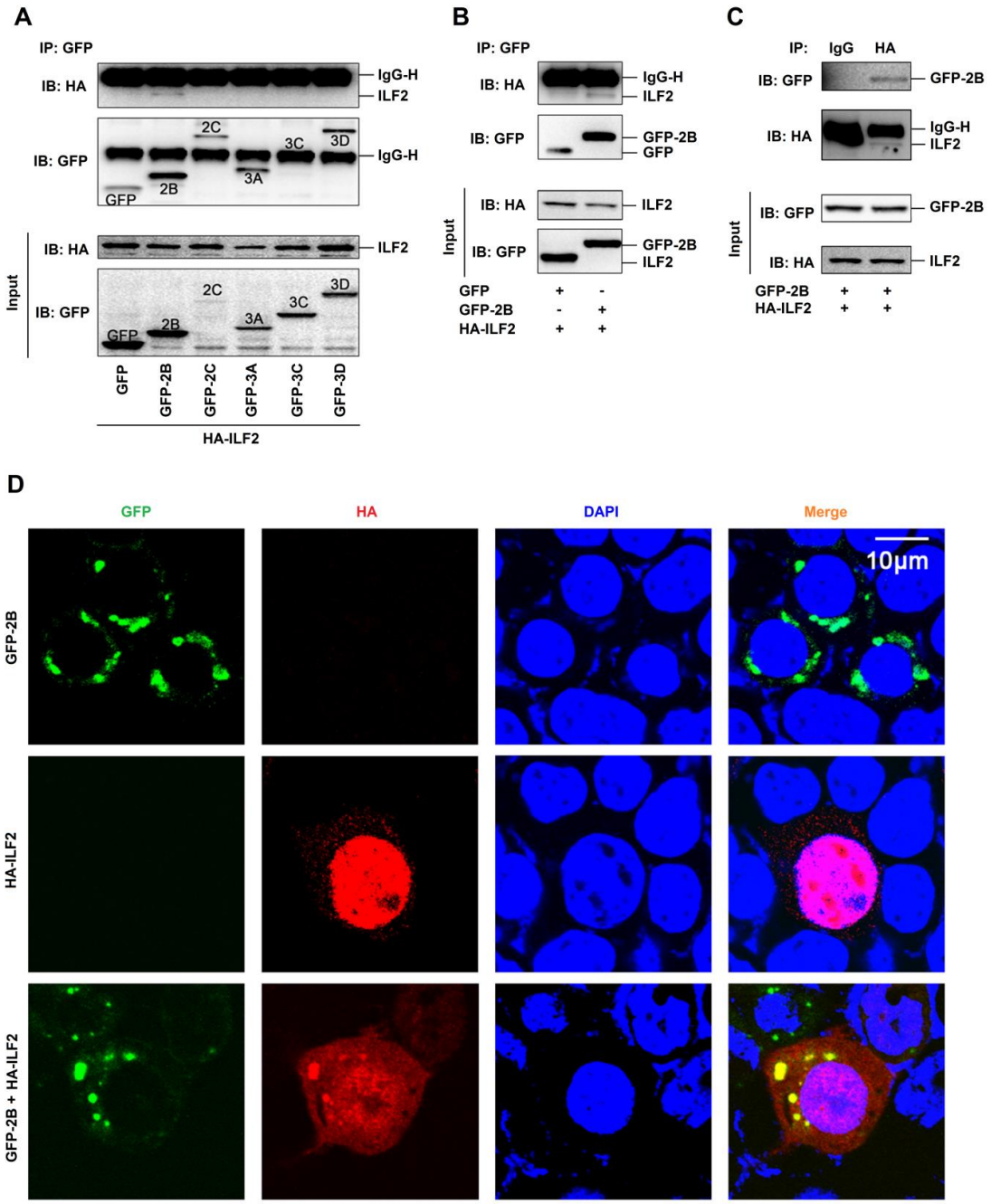

Figure 4. EV71 2B interacts and co-localizes with ILF2 in the cytoplasm. (**A**) Human embryonic kidney (HEK293T) cells were co-transfected with plasmid encoding HA-ILF2 and plasmids encoding each of EV71 non-structure proteins, GFP-2B, GFP-2C, GFP-3A, GFP-3C, and GFP-3D, respectively. The GFP-tag, GFP-2B, GFP-2C, GFP-3A, GFP-3C, GFP-3D, and HA-ILF2 proteins were subjected to Co-immunoprecipitation (Co-IP) assay with anti-GFP antibody or with IgG as a negative control. The levels of GFP-tag, GFP-2B, GFP-2C, GFP-3A, GFP-3C, GFP-3D, and HA-ILF2 proteins were detected by Western-blot analyses using anti-GFP antibody or anti-HA antibody, as indicated. (**B** and **C**) HEK293T cells were co-transfected with pHA-ILF2 and pGFP-tag or pGFP-2B. The GFP-tag, GFP-2B, and HA-ILF2 proteins were subjected to Co-IP assay with anti-GFP antibody (B). The GFP-tag, GFP-2B, and HA-ILF2 proteins were subjected to Co-IP assay with anti-HA antibody or with IgG as a negative control (C). The levels of GFP-tag, GFP-2B, and HA-ILF2 proteins were measured by Western-blot using anti-GFP antibody or anti-HA antibody, as indicated. (**D**) HEK293T cells were transfected with pGFP-2B alone or pHA-ILF2 alone or co-transfected with pGFP-2B and pHA-ILF2

together. The localization and distribution of EV71 2B protein (green), ILF2 protein (red), and the nuclei (blue) were visualized under Laser scanning confocal microscope.

4. Discussion

EV71 infection causes HFMD, lymphopenia, herpetic pharyngitis, and neurological diseases, including brain stemencephalitis, aseptic meningitis, acute flaccid paralysis, poliomyelitis-like paralysis, and acute flaccid paralysis [39–42]. Therefore, it is important to study the mechanisms by which the host regulates EV71 infection and the virus antagonizes host-mediated antiviral effects. In this study, we initially reveal that ILF2 down-regulates EV71 TCID50, attenuates EV71 PFU, thereby repressing EV71 infection. Although this result is similar with previous reports showing that ILF2 regulates the replication of other viruses [28–33], our study provides the first evidence that ILF2 represses EV71 infection. Although ILF2 plays critical roles in the repression of viral infection, the mechanism by which virus antagonizes ILF2-mediated antiviral effects has not been revealed until this study. ILF2 mRNA expression and protein production are repressed upon EV71 infection in THP-1 differentiated macrophages and RD cells. Additionally, EV71 2B interacts with ILF2 to facilitate ILF2 translocation from nucleus to cytoplasm and co-localize with 2B in the cytoplasm.

EV71 2B is involved in the viral RNA replication [7], activates the mitochondrial cell death pathway [8], and enhances viral release [9]. This study reveals a new role of 2B in the regulation of ILF2. Previous study reported that 2B attenuates RIG-I-mediated antiviral effects through repression RIG-I expression [10]. We demonstrate that 2B antagonizes ILF2-mediated antiviral effects by repressing ILF2 expression and through interesting with ILF2 to promote its translocation from nucleus to cytoplasm, thereby altering ILF2 function. Since ILF2 is a transcription factor that mainly locates and functions in the nucleus [33], EV71 2B-mediated ILF2 translocation from the nucleus to the cytoplasm must lead to the inhibition of ILF2 function.

In conclusions, we reveal a distinct mechanism by which EV71 antagonizes ILF2-mediated antiviral effects by inhibiting ILF2 expression and promoting ILF2 translocation from the nucleus to cytoplasm through 2B protein.

Author Contributions: Data curation, J.J., W.W., S.A., Q.T., K.W., Y.L. and J.W.; Funding acquisition, J.W.; Methodology, W.W., S.A., Q.T., K.W. and Y.L.; Project administration, Q.T., K.W. and Y.L.; Resources, Q.T., K.W. and Y.L.; Supervision, J.W.; Writing - original draft, J.J., W.W. and J.W.; Writing - review and editing, J.J., W.W. and J.W.

Funding: This work was supported by National Natural Science Foundation of China (81730061 and 31800147), and Guangdong Province "Pearl River Talent Plan" Innovation and Entrepreneurship Team Project (2017ZT07Y580).

Conflicts of Interest: The authors declare no conflict of interest.

References

1. Solomon, T., Lewthwaite, P., Perera, D., Cardosa, M.J., McMinn, P., Ooi, M.H. Virology, epidemiology, pathogenesis, and control of enterovirus 71. *Lancet. Infect. Dis.* **2010**, *10*, 778–790.
2. Huang, P.N., and Shih, S.R. Update on enterovirus 71 infection. *Curr. Opin. Virol.* **2014**, *5*, 98–104.
3. Ooi, M.H., Wong, S.C., Lewthwaite, P., Cardosa, M.J., Solomon, T. Clinical features, diagnosis, and management of enterovirus 71. *Lancet Neurol.* **2010**, *9*, 1097–1105.
4. Weng, K.F., Chen, L.L., Huang, P.N., Shih, S.R. Neural pathogenesis of enterovirus 71 infection. *Microbes infect.* **2010**, *12*, 505–510.
5. Brown, B.A., Pallansch, M.A. Complete nucleotide sequence of enterovirus 71 is distinct from poliovirus. *Virus Res.* **1995**, *39*, 195–205.
6. McMinn, P.C. An overview of the evolution of enterovirus 71 and its clinical and public health significance. *FEMS Microbiol. Rev.* **2002**, *26*, 91–107.
7. Xie, S., Wang, K., Yu, W., Lu, W., Xu, K., Wang, J., Ye, B, Schwarz W, Jin Q, Sun B. DIDS blocks a chloride-dependent current that is mediated by the 2B protein of enterovirus 71. *Cell Res.* **2011**, *21*, 1271–1215.

8. Cong, H., Du, N., Yang, Y., Song, L., Zhang, W., Tien, P. Enterovirus 71 2B induces cell apoptosis by directly inducing the conformational activation of the proapoptotic protein Bax. *J. Virol.* **2016**, *90*, 9862–9877.
9. Ao, D., Guo, H.C., Sun, S.Q., Sun, D.H., Fung, T.S., Wei, Y.Q., Han, S.C., Yao, X.P., Cao, S.Z., Liu, D.X.; et al., Viroporin activity of the foot-and-mouth disease virus non-structural 2B protein. *PLoS One* **2015**, *10*, e0125828.
10. Zhu, Z., Wang, G., Yang, F., Cao, W., Mao, R., Du, X., Zhang, X., Li, C., Li, D., Zhang, K.; et al., Foot-and-mouth disease virus viroporin 2B antagonizes RIG-I-mediated antiviral effects by inhibition of its protein expression. *J. Virol.* **2016**, *90*, 11106–11121.
11. Kao PN, Chen L, Brock G, Ng J, Kenny J, Smith AJ, Corthésy B. Cloning and expression of cyclosporin A- and FK506-sensitive nuclear factor of activated T-cells: NF45 and NF90. *J. Biol. Chem.* **1994**, *269*, 20691–20699.
12. Shamanna, R.A., Hoque, M., Lewis-Antes, A., Azzam, E.I., Lagunoff, D., Pe'ery, T., Mathews, M.B. The NF90/NF45 complex participates in DNA break repair via nonhomologous end joining. *Mol. Cell Biol.* **2011**, *31*, 4832–4843.
13. Karmakar, S., Mahajan, M.C., Schulz, V., Boyapaty, G., Weissman, S.M. A multiprotein complex necessary for both transcription and DNA replication at the beta-globin locus. *EMBO J.* **2010**, *29*, 3260–3271.
14. Kiesler, P., Haynes, P.A., Shi, L., Kao, P.N., Wysocki, V.H., Vercelli, D. NF45 and NF90 regulate HS4-dependent interleukin-13 transcription in T cells. *J. Biol, Chrm.* **2010**, *285*, 8256–8267.
15. Graber, T.E., Baird, S.D., Kao, P.N., Mathews, M.B., Holcik, M. NF45 functions as an IRES trans-acting factor that is required for translation of cIAP1 during the unfolded protein response. *Cell Death Differ.* **2010**, *17*, 719–729.
16. Faye, M.D., Graber, T.E., Liu, P., Thakor, N., Baird, S.D., Durie, D., Holcik, M. Nucleotide composition of cellular internal ribosome entry sites defines dependence on NF45 and predicts a posttranscriptional mitotic regulon. *Mol. Cell Biol.* **2013**, *33*, 307–318.
17. Marchesini, M., Ogoti, Y., Fiorini, E., Aktas Samur, A., Nezi, L., D'Anca, M., Storti, P., Samur, M.K., Ganan-Gomez, I., Fulciniti, M.T.; et al., ILF2 Is a regulator of RNA splicing and DNA damage response in 1q21-amplified multiple myeloma. *Cancer Cell* **2017**, *32*, 88–100.
18. Sakamoto, S., Aoki, K., Higuchi, T., Todaka, H., Morisawa, K., Tamaki, N., Hatano, E., Fukushima, A., Taniguchi, T., Agata, Y. The NF90-NF45 complex functions as a negative regulator in the microRNA processing pathway. *Mol. Cell Biol.* **2009**, *29*, 3754–3769.
19. Todaka, H., Higuchi, T., Yagyu, K., Sugiyama, Y., Yamaguchi, F., Morisawa, K., Ono, M., Fukushima, A., Tsuda, M., Taniguchi, T.; et al. Overexpression of NF90-NF45 represses Myogenic microRNA biogenesis, resulting in development of skeletal muscle atrophy and centronuclear muscle fibers. *Mol. Cell Biol.* **2015**, *35*, 2295–2308.
20. Higuchi, T., Todaka, H., Sugiyama, Y., Ono, M., Tamaki, N., Hatano, E., Takezaki, Y., Hanazaki, K., Miwa, T., Lai, S.; et al. Suppression of microRNA-7 (miR-7) biogenesis by nuclear factor 90-nuclear factor 45 complex (NF90-NF45) controls cell proliferation in hepatocellular carcinoma. *J. Biol. Chem.* **2016**, *291*, 21074–21084.
21. Wan, C., Gong, C., Ji, L., Liu, X., Wang, Y., Wang, L., Shao, M., Yang, L., Fan, S., Xiao, Y., et al. NF45 overexpression is associated with poor prognosis and enhanced cell proliferation of pancreatic ductal adenocarcinoma. *Mol. Cell. Biochem.* **2015**, *410*, 25–35.
22. Bi, Y., Shen, W., Min, M., Liu, Y. MicroRNA-7 functions as a tumor-suppressor gene by regulating ILF2 in pancreatic carcinoma. *Int. J. Mol. Med.* **2017**, *39*, 900–906.
23. Cheng, S., Jiang, X., Ding, C., Du, C., Owusu-Ansah, K.G., Weng, X., Hu, W., Peng, C., Lv, Z., Tong, R., et al., Expression and critical role of interleukin enhancer binding factor 2 in hepatocellular carcinoma. *Int. J. Mol. Sci.* **2016**, *17*, E1373.
24. Ni, T., Mao, G., Xue, Q., Liu, Y., Chen, B., Cui, X., Lv, L., Jia, L., Wang, Y., Ji, L. Upregulated expression of ILF2 in non-small cell lung cancer is associated with tumor cell proliferation and poor prognosis. *J. Mol. Histol.* **2015**, *46*, 325–335.

25. Ni, S., Zhu, J., Zhang, J., Zhang, S., Li, M., Ni, R., Liu, J., Qiu, H., Chen, W., Wang, H., et al., Expression and clinical role of NF45 as a novel cell cycle protein in esophageal squamous cell carcinoma (ESCC). *Tumour Biol.* **2015**, *36*, 747–756.
26. Yin, Z.H., Jiang, X.W., Shi, W.B., Gui, Q.L., Yu, D.F. Expression and clinical significance of ILF2 in gastric cancer. *Dis. Markers* **2017**, *2017*, 4387081.
27. Jin, Z., Xu, L., Zhang, L., Zhao, M., Li, D., Ye, L., Ma, Y., Ren, S., Yu, H., Wang, D., et al., Interleukin enhancer binding factor 2 is a prognostic biomarker for breast cancer that also predicts neoadjuvant chemotherapy responses. *Am. J. Transl. Res.* **2018**, *10*, 1677–1689.
28. Li, Y., Belshan, M. NF45 and NF90 bind HIV-1 RNA and modulate HIV gene expression. *Viruses* **2016**, *8*, E47.
29. Isken, O., Baroth, M., Grassmann, C.W., Weinlich, S., Ostareck, D.H., Ostareck-Lederer, A., Behrens, S.E., et al. Nuclear factors are involved in hepatitis C virus RNA replication. *RNA* **2007**, *13*, 1675–1692.
30. Merrill, M.K., Gromeier, M. The double-stranded RNA binding protein 76:NF45 heterodimer inhibits translation initiation at the rhinovirus type 2 internal ribosome entry site. *J Virol.* **2006**, *80*, 6936–6942.
31. Huang, Y., Wang, W., Xu, Z., Pan, J., Zhao, Z., Ren, Q. Eriocheir sinensis microRNA-7 targets crab Myd88 to enhance white spot syndrome virus replication. *Fish Shellfish Immunol.* **2018**, *79*, 274–283.
32. Shamanna, R.A., Hoque, M., Pe'ery, T., Mathews, M.B. Induction of p53, p21 and apoptosis by silencing the NF90/NF45 complex in human papilloma virus-transformed cervical carcinoma cells. *Oncogene* **2013**, *32*, 5176–5185.
33. Wen, X., Bian, T., Zhang, Z., Zhou, L., Ge, X., Han, J., Guo, X., Yang, H., Yu, K. Interleukin-2 enhancer binding factor 2 interacts with the nsp9 or nsp2 of porcine reproductive and respiratory syndrome virus and exerts negatively regulatory effect on the viral replication. *Virol. J.* **2017**, *14*, 125.
34. Wang, W., Xiao, F., Wan, P., Pan, P., Zhang, Y., Liu, F., Wu, K., Liu, Y., Wu, J. EV71 3D protein binds with NLRP3 and enhances the assembly of inflammasome complex. *PLoS Pathog.* **2017**, *13*, e1006123.
35. Jin, J., Li, A., Wang, W., Wu, J. Interleukin-enhanced binding factor 2 interacts with NLRP3 to inhibit the NLRP3 inflammasome activation. *Biochem. Biophys. Res. Commun.* **2018**, *500*, 398–404.
36. Luo, Z., Ge, M., Chen, J., Geng, Q., Tian, M., Qiao, Z., Bai, L., Zhang, Q., Zhu, C., Xiong, Y., et al. HRS plays an important role for TLR7 signaling to orchestrate inflammation and innate immunity upon EV71 infection. *PLoS Pathog.* **2017**, *13*, e1006585.
37. Park, E.K., Jung, H.S., Yang, H.I., Yoo, M.C., Kim, C., Kim, K.S. Optimized THP-1 differentiation is required for the detection of responses to weak stimuli. *Inflamm. Res.* **2007**, *56*, 45–50.
38. Wang, W., Li, G., Wu, D., Luo, Z., Pan, P., Tian, M., Wang, Y., Xiao, F., Li, A., Wu, K. Zika virus infection induces host inflammatory responses by facilitating NLRP3 inflammasome assembly and interleukin-1beta secretion. *Nat. Commun. 2018*, **9**, *106*.
39. Wang, S.M., Lei, H.Y., Huang, M.C., Su, L.Y., Lin, H.C., Yu, C.K., Wang, J.L., Liu, C.C. Modulation of cytokine production by intravenous immunoglobulin in patients with enterovirus 71-associated brainstem encephalitis. *J. Clin. Virol.* **2006**, *37*, 47–52.
40. Gong, X., Zhou, J., Zhu, W., Liu, N., Li, J., Li, L., Jin, Y., Duan, Z. Excessive proinflammatory cytokine and chemokine responses of human monocyte-derived macrophages to enterovirus 71 infection. *BMC Infect. Dis.* **2012**, *12*, 224.
41. Griffiths, M.J., Ooi, M.H., Wong, S.C., Mohan, A., Podin, Y., Perera, D., Chieng, C.H., Tio, P.H., Cardosa, M.J., Solomon, T. In enterovirus 71 encephalitis with cardio-respiratory compromise, elevated interleukin 1β, interleukin 1 receptor antagonist, and granulocyte colony-stimulating factor levels are markers of poor prognosis. *J. Infect. Dis.* **2012**, *206*, 881–892.
42. Weng, K.F., Chen, L.L., Huang, P.N., Shih, S.R. Neural pathogenesis of enterovirus 71 infection. *Microbes Infect.* **2010**, *12*, 505–510.